Gluon condensation: From nucleon to Galactic Center

Wei Zhu,[1,*] Zi-Qing Xia,[2] Yu-Chen Tang,[2] and Lei Feng[2]

[1]*Department of Physics, East China Normal University, Shanghai 200241, People's Republic of China*
[2]*Key Laboratory of Dark Matter and Space Astronomy, Purple Mountain Observatory, Chinese Academy of Sciences, Nanjing 210008, People's Republic of China*

(Received 27 April 2023; accepted 4 December 2023; published 21 December 2023)

The Galactic Center excess (GCE), one of the most remarkable discoveries by Fermi-LAT, has prompted extensive exploration over the past decade, often attributed to dark matter or millisecond pulsars. This work proposes a novel interpretation on the origin of the GCE, focusing on the observed spectral shape. Protons are accelerated at the Galactic Center and collide with the neutron cluster on the surface of the nonrotating neutron stars. Due to the gluon condensation in nucleons, these collisions produce a large number of mesons, which have reached to the saturation state and subsequently generate the broken power law in the gamma ray spectra. We explained the spectral shape of GCE using the gluon condensation and an assumption of existing the nonrotating neutron stars at the Galactic Center. This example of the gluon condensation mechanism not only expands the applications of the hadronic scenario in the cosmic gamma ray spectra but also provides a new evidence of the gluon condensation.

DOI: 10.1103/PhysRevD.108.123035

I. INTRODUCTION

The Galactic Center is a hub of high-density matter, comprised of neutron stars, black holes and enigmatic dark matter. This environment presents an exceptional opportunity for astronomers and physicists to study astrophysical objects in a highly compacted region. The Fermi Large Area Telescope (Fermi-LAT) has detected an excess of gamma rays originating from the Galactic Center [1–3], known as the Galactic Center excess (GCE). The GCE is a highly intriguing mystery in astrophysics, and deciphering the physical processes behind this phenomenon presents a challenge [4,5].

Early investigations have indicated that one of the possible GCE sources origins from the annihilation of weakly interacting massive particles (WIMPs), which is one of the leading dark matter candidates. Meanwhile, the GCE spectra bear resemble to the GeV gamma-ray spectra observed in pulsars, despite the identity of their progenitor pulsars remaining unclear.

A difficult problem is that the GCE spectra are significantly influenced by the Galactic diffuse emission [6–13]. It is critical to eliminate these contributions from the GCE spectra. Recently, Dinsmore and Slatyer utilized a generalized Navarro-Frenk-White squared spatial template to model pulsar distributions in the Galactic Center region and extracted the corresponding GCE flux from nine previous GCE energy spectra [14]. The region of interest (ROI) used by them was a square region selected by Galactic latitudes $|b| < 20°$ and Galactic longitudes $|l| < 20°$, with a mask of the Galactic plane with $|b| < 2°$. The nine inferred GCE spectra in [14] show some differences from each other due to different fitting approaches, ROI choices, signal models and background templates. However, unexpectedly, all nine GCE spectra exhibit strong evidence of the typical broken power law (BPL) shape. This consistent presence of the BPL shape across the diverse GCE spectra, despite the complexities introduced by different analyses and modeling approaches, introduces a tantalizing puzzle that beckons for a deeper comprehension of the underlying physical processes driving the GCE.

This article attempts to attribute the observed GCE spectra in Fig. 1 to the gluon condensation effect in nucleon (proton and neutron). As we know, high energy nucleon collisions are general processes in the Galactic Center. The hadronic scenario of gamma-ray emission is such $pp \to \pi^0 \to 2\gamma$, where a bump of energy spectrum near ~1 GeV (i.e. the "π-bump") origins from a peak in π^0 decay [15], while the gluon distributions in nucleon dominate the π-yield N_π at high energy [16]. The evolution equations in quantum chromodynamics (QCD) predict that the gluon distributions may smoothly tend toward an equilibrium state between the splitting and fusion of gluons, known as the color glass condensation (CGC) [17]. Following them, one of us (W.Z.) first proposed that the CGC distributions will continually evolve and result in a chaotic solution [18–21]. This leads to dramatic chaotic oscillations that cause strong shadowing and antishadowing effects, forcing a large number of soft gluons to condense into a state at a critical momentum (x_c, k_c), where x_c is a

*Corresponding author: wzhu@phy.ecnu.edu.cn

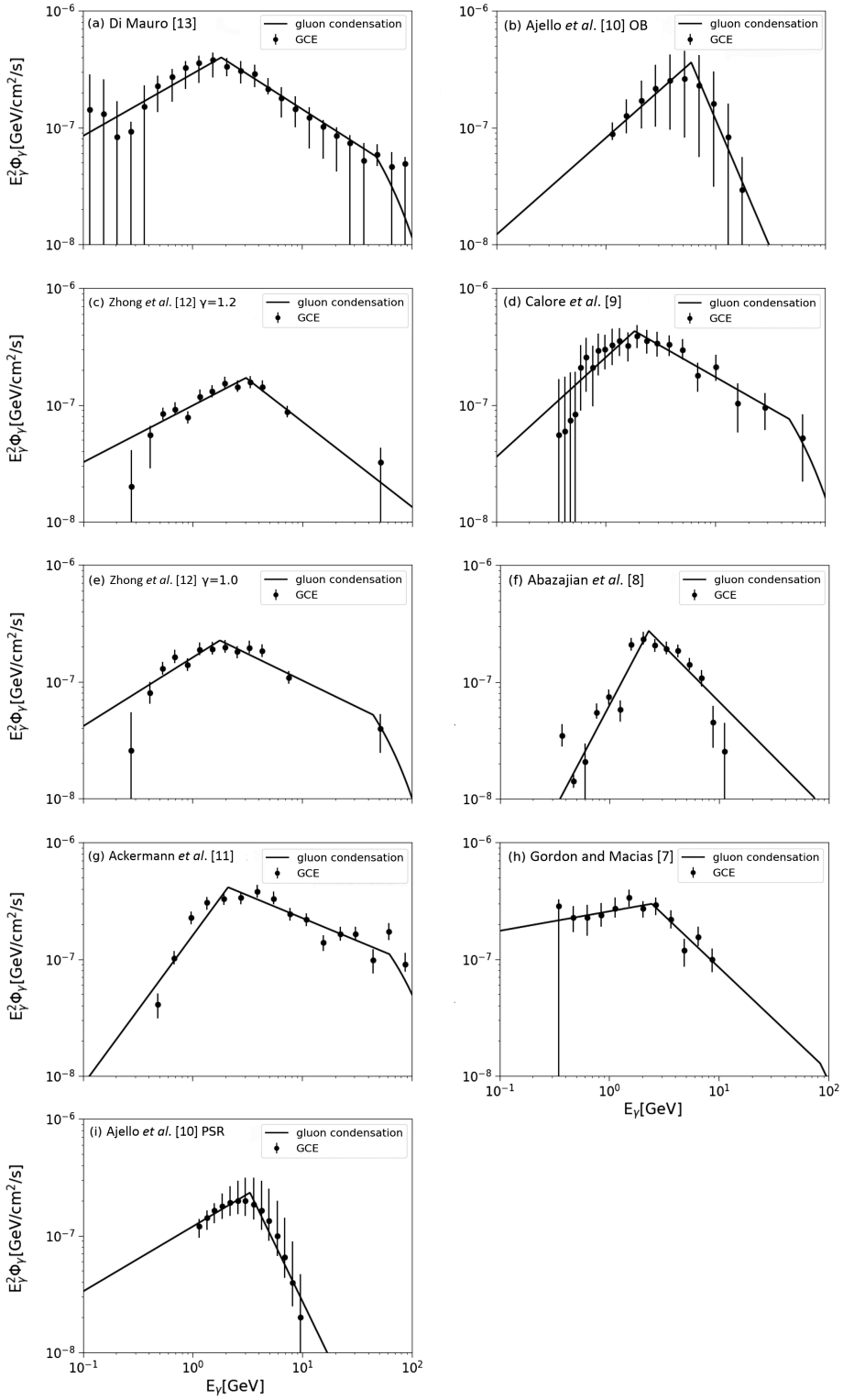

FIG. 1. The GCE-spectra predicted by the gluon condensation mechanism. The data are taken from [6–14]. The results show the broken power law.

fraction of the proton's longitudinal momentum carried by the condensed gluon and k_c is their transverse momentum. This is the gluon condensation (Fig. 2). We will illustrate in Sec. II that the sharp peak in the gluon distributions can significantly enhance the cross section of the nucleon collisions and results a new bump in the gamma ray spectra, which is stronger than the "π-bump" and has a typical BPL form with an exponential suppression factor.

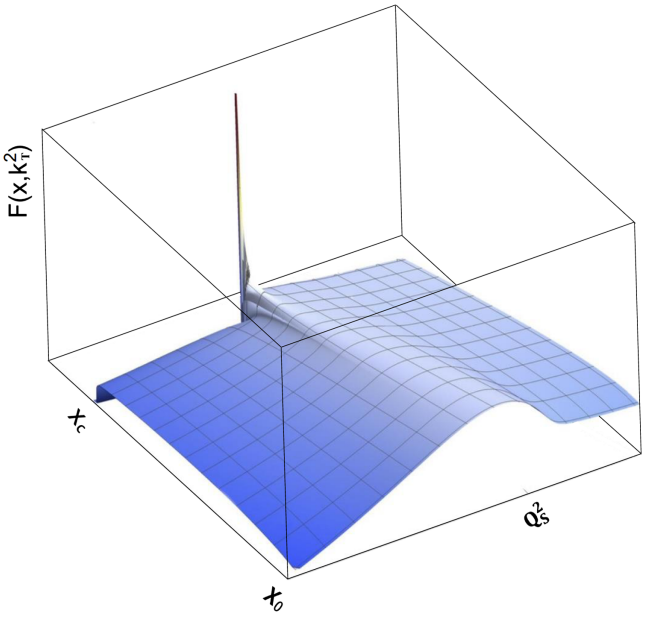

FIG. 2. A schematic solution of a QCD evolution equation [21], which shows the evolution of transverse momentum dependent distribution $F(x, k_T^2)$ of gluons in nucleon from the CGC at x_0 to the gluon condensation at x_c. Note that all gluons with $x < x_c$ are stacked at (x_c, k_c).

Using the gluon condensation mechanism, we will explain the GCE spectra in Sec. III. We find that not only in the spectral shape but also in the range of model parameters, the GCE and the millisecond pulsar spectra are similar. It implies that all of them originate from the same emission mechanism, i.e., the collision of high energy proton with the big neutron cluster $A^* \gg 300$ (A^* is the number of neutrons) on the surface of a neutron star.

However, there are not enough observed pulsar spectra to fully cover the GCE curve. Moreover, even if enough millisecond pulsars are discovered in the Galactic Center, it is difficult to synthesize a single BPL spectrum from a set of BPL distributions with diverse spectral parameters. One solution to this problem is to assume the existence of a large population of nonrotating (including slower rotating) neutron stars at the Galactic Center. Although the nonrotating neutron stars are one of the theoretical topics in nuclear physics and astronomy, their observational data are extremely rare since the lack of their characteristic radiation spectra. The gluon condensation mechanism of the GCE may arouse interest in the nonrotating neutron stars.

The information about the GCE consists of spectral shape and its spatial morphology, the latter being related to the spatial distribution of the nonrotating stars in the Galactic Center. The explanation of GCE requires confirmation not only in terms of its spectrum but also in its spatial distribution. Unfortunately, there is no observation on the nonrotating neutron stars due to lack of detectable effects except the gluon condensation. We simply assume that the spatial distribution of the nonrotating neutron stars are similar to the millisecond pulsars, as given in Sec. IV. Finally, in the last section, we give discussions and a brief summary.

II. THE GLUON CONDENSATION MECHANISM

In the hadronic scenario, cosmic gamma rays can be generated through the process $pp \to \pi^0 \to 2\gamma$ and they are calculated by [22]

$$\Phi_\gamma(E_\gamma) = C_\gamma \left(\frac{E_\gamma}{\mathrm{GeV}}\right)^{-\beta_\gamma} \int_{E_\pi^{\min}}^{E_\pi^{\mathrm{cut}}} dE_\pi \left(\frac{E_p}{\mathrm{GeV}}\right)^{-\beta_p} \times N_\pi(E_p, E_\pi) \frac{d\omega_{\pi-\gamma}(E_\pi, E_\gamma)}{dE_\gamma}, \quad (1)$$

where the spectral index β_γ includes the photon loss due to the medium absorption of pions. The accelerated protons obey a power law $N_p \sim E_p^{-\beta_p}$ in the source. C_γ incorporates the kinematic factor and the flux dimension.

On the other hand, according to the hadronic collisions model, about the half energies of parent protons are taken away by the valence quarks, which form the leading particles, and the remaining energies are transformed into the secondary hadrons (mainly pions) in the central region through gluon interactions. The cross section of an inclusive particle production in high-energy proton-proton collision is dominated by the production of gluon minijet using the unintegrated gluon distribution via [23,24]

$$\frac{dN_g}{dk_T^2 dy} = \frac{64N_c}{(N_c^2-1)k_T^2} \int_{q_{T,\min}}^{q_{T,\max}} q_T dq_T \int_0^{2\pi} d\phi \alpha_s(\Omega) \times \frac{F\left(x_1, \frac{1}{4}(k_T+q_T)^2\right) F\left(x_2, \frac{1}{4}(k_T-q_T)^2\right)}{(k_T+q_T)^2 (k_T-q_T)^2}, \quad (2)$$

where k_T and q_T are the transverse momenta, $\Omega = Max\{k_T^2, (k_T+q_T)^2/4, (k_T-q_T)^2/4\}$ and the longitudinal momentum fractions of interacting gluons are fixed by kinematics $x_{1,2} = k_T e^{\pm y}/\sqrt{s}$.

A key step is how to calculate $N_g \to N_\pi$ at $pp \to \pi$, which involves unknown nonperturbative QCD effects. Fortunately, a steep and high peak in the gluon distributions can determine $N_\pi(E_\pi, E_p)$ and lead to a typical BPL spectrum as shown in Fig. 1. Let us to repeat this simple derivation in [25–27].

Experiments show that N_π increases as the collision energy increases, because more gluons participate in the process of making new particles. So when a significant amount of condensed gluons at the threshold x_c suddenly participate in the pp-collisions, it inevitably results in a large number of secondary meson production dramatically. However, since meson has mass, their yield N_π is limited. As a limiting case, we imagine that N_π reaches its maximum value due to the gluon condensation effect, i.e., almost all available kinetic energies of collisions at the center-of-mass (c.m.) frame are used to create pions. Of course, the validity

of this approximation will be tested by the following observed data. By taking this limit, we can avoid the complicated hadronization mechanism and write energy conservation

$$E_p + m_p = \tilde{m}_p\gamma_1 + \tilde{m}_p\gamma_2 + N_\pi m_\pi \gamma, \tag{3}$$

where $\tilde{m}_p$ marks the leading particle and γ_i is the Lorentz factor. The square of relativistic invariant total energy $s = (p_1 + p_2)^2$ in the laboratory (Lab) frame and the c.m. frame are

$$2m_p^2 + 2E_p m_p = (2\tilde{E}_p^* + N_\pi m_p)^2. \tag{4}$$

Using

$$2\tilde{E}_p^* \equiv \left(\frac{1}{k} - 1\right) N_\pi m_\pi, \tag{5}$$

$k \simeq 1/2$ is an inelastic factor and it is irrelevant to the system, we have

$$\tilde{m}_p\gamma_1 + \tilde{m}_p\gamma_2 = \left(\frac{1}{k} - 1\right) N_\pi m_\pi \gamma. \tag{6}$$

From Eqs. (3) and (4) we have the power law for N_π

$$\ln N_\pi = 0.5\ln(E_p/\mathrm{GeV}) + a, \quad \ln N_\pi = \ln(E_\pi/\mathrm{GeV}) + b, \quad \text{with } E_\pi \in [E_\pi^{\mathrm{GC}}, E_\pi^{\mathrm{cut}}], \tag{7}$$

where $a \equiv 0.5\ln(2m_p/\mathrm{GeV}) - \ln(m_\pi/\mathrm{GeV}) + \ln k$ and $b \equiv \ln(2m_p/\mathrm{GeV}) - 2\ln(m_\pi/\mathrm{GeV}) + \ln k$.

Submitting Eq. (7) into Eq. (1), one can analytically obtain (here we neglect the simple integral calculations)

$$E_\gamma^2 \Phi_\gamma^{\mathrm{GC}}(E_\gamma) \simeq \begin{cases} \frac{2e^b C_\gamma}{2\beta_p - 1}(E_\pi^{\mathrm{GC}})^3 \left(\frac{E_\gamma}{E_\pi^{\mathrm{GC}}}\right)^{-\beta_\gamma + 2} & \text{if } E_\gamma \le E_\pi^{\mathrm{GC}}, \\ \frac{2e^b C_\gamma}{2\beta_p - 1}(E_\pi^{\mathrm{GC}})^3 \left(\frac{E_\gamma}{E_\pi^{\mathrm{GC}}}\right)^{-\beta_\gamma - 2\beta_p + 3} & \text{if } E_\pi^{\mathrm{GC}} < E_\gamma < E_\pi^{\mathrm{cut}}, \\ \frac{2e^b C_\gamma}{2\beta_p - 1}(E_\pi^{\mathrm{GC}})^3 \left(\frac{E_\gamma}{E_\pi^{\mathrm{GC}}}\right)^{-\beta_\gamma - 2\beta_p + 3} \exp\left(-\frac{E_\gamma}{E_\pi^{\mathrm{cut}}} + 1\right) & \text{if } E_\gamma \ge E_\pi^{\mathrm{cut}}, \end{cases} \tag{8}$$

This is the gluon condensation spectrum. A phenomenological exponential cut factor in Eq. (8) describes the fast suppression of the energy spectrum at $E_\gamma > E_\pi^{\mathrm{cut}}$. The reason is that the gluons at $x < x_c$ have been condensed at x_c and where no gluons to participate the pA interaction. Thus, E_γ has a upper limit E_π^{cut} in Eq. (1).

Additionally, the two energy scales, E_π^{GC} and E_π^{cut} have the following relation.

$$E_\pi^{\mathrm{cut}} = \beta e^{b-a}\sqrt{\frac{2m_p}{k_c^2}}(E_\pi^{\mathrm{GC}})^2, \tag{9}$$

where $\beta = 1$ if $E_\pi^{\mathrm{GC}} \ll 100$ GeV. Note that all energies take the GeV-unit and

$$E_p = \frac{2m_p}{m_\pi^2} E_\pi^2 \tag{10}$$

gives the energy of incident proton corresponding to E_π in the Lab frame.

We emphasize that the BPL in Eq. (8) is the analytic solution of the gluon condensation mechanism, rather than the mathematical parametrized formula in the literature. The former has its QCD foundation and a clear physical picture, while the latter is generally used in the data descriptions. Equation (8) has been used to study the sub-TeV gamma-ray spectra of the active Galactic nuclei (AGNs) and the very high energy (VHE) gamma ray spectra of pulsars, especially, the latter shows a similar structure with the GCE.

III. THE GCE SPECTRA IN THE GLUON CONDENSATION MECHANISM

We use the gluon condensation spectrum Eq. (8) to fit all nine examples in Fig. 1, where the data are extracted by work [6–14]. Note that E_π^{cut} in Figs. 1(b), 1(c), 1(f), 1(h), and 1(i) are beyond the coordinate range according to Eq. (9). The parameters are listed in Table I. It is interesting to note that these parameters are broadly consistent with the fitting results of the same gluon condensation mechanism in the GeV gamma ray spectra of pulsars in [28]. It seems that the GCE and the GeV gamma-ray spectra of pulsars may have the same origin.

The gluon condensation threshold E_π^{GC} is the target-dependent. According to the uncertainty relation, when a nucleus participates in collisions, the gluons with small x from different nucleons can fusion and enhancing the nonlinear effect. Due to kinematic constraints, when protons collide, not all gluons are excited to participate in the interaction. The higher the proton collision energy, the smaller x of the excited gluons. Therefore, a very high collision energy is required for the process of producing mesons by a large number of gluons condensing at a small critical x_c. The study of QCD evolution equations shows that the larger A, the stronger the nonlinear effect and the larger the critical x_c for generating the lower condensation

TABLE I. The parameters of the GCE spectra in the gluon condensation mechanism.

GCE spectrum	$E_\pi^{\rm GC}$ (GeV)	$C_\gamma(\mathrm{GeV}^{-2}\,\mathrm{cm}^{-2}\,\mathrm{s}^{-1})$	β_p	β_γ	χ^2/d.o.f.
Di Mauro [13]	1.86 ± 0.0008	$6.53 \times 10^{-10} \pm 1.45 \times 10^{-10}$	1.06 ± 0.08	1.49 ± 0.12	$5.36/20 = 0.27$
Ajello *et al.* [10] OB	6.07 ± 1.55	$4.77 \times 10^{-11} \pm 3.82 \times 10^{-11}$	2.03 ± 0.11	1.17 ± 0.34	$0.42/6 = 0.07$
Zhong *et al.* [12] $\gamma = 1.2$	3.06 ± 0.35	$7.00 \times 10^{-11} \pm 2.36 \times 10^{-11}$	1.11 ± 0.10	1.51 ± 0.08	$10.75/9 = 1.19$
Calore *et al.* [9]	1.83 ± 0.12	$1.00 \times 10^{-9} \pm 5.08 \times 10^{-10}$	1.23 ± 0.10	1.07 ± 0.14	$5.87/18 = 0.33$
Zhong *et al.* [12] $\gamma = 1.0$	1.78 ± 0.21	$4.01 \times 10^{-10} \pm 1.63 \times 10^{-10}$	1.02 ± 0.07	1.41 ± 0.11	$12.84/9 = 1.43$
Abazajian *et al.* [8]	2.23 ± 0.12	$6.59 \times 10^{-10} \pm 1.20 \times 10^{-10}$	1.89 ± 0.08	0.16 ± 0.11	$42.71/11 = 3.88$
Ackermann *et al.* [11]	2.12 ± 0.15	$6.95 \times 10^{-10} \pm 1.65 \times 10^{-10}$	1.34 ± 0.06	0.71 ± 0.11	$34.25/12 = 2.85$
Gordon and Macias [7]	2.42 ± 0.51	$2.10 \times 10^{-10} \pm 1.52 \times 10^{-10}$	1.02 ± 0.14	1.84 ± 0.16	$4.60/8 = 0.58$
Ajello *et al.* [10] PSR	3.38 ± 0.56	$1.57 \times 10^{-10} \pm 9.57 \times 10^{-11}$	1.81 ± 0.35	1.41 ± 0.29	$0.82/10 = 0.08$

threshold $E_\pi^{\rm GC}$. Specifically, the numerical computations show that the values of $E_\pi^{\rm GC}$ are taken from 0.1 TeV ∼ 20 TeV in the pA collisions if target A taking from heavy nucleus to proton (see Fig. 11 in [29]). Neutron star provides a completely new energy range for observing the gluon condensation effect since $A^* \gg A$.

Table I shows that $E_\pi^{\rm GC} \sim 1$ GeV, which are consistent with that in the millisecond pulsars [28]. It is conceivable that the surface of a neutron star has a lattice structure formed by heavy atoms, while the density of neutrons is significantly higher than that of atoms. The superfluid of neutrons inside the interior can penetrate the lattice space since there is sufficient empty space among the atoms, resulting in the formation of neutron cluster A^* on the star surface. We assume that these neutron clusters A^* are stable. Due to these lattices having a similar size, the gluon condensation threshold $E_\pi^{\rm GC}$ are restricted to a similar low energy scale. Therefore, we consider that the GCE originates from the collisions of VHE protons in the Galactic Center with the neutron cluster A^* on the surface of neutron stars.

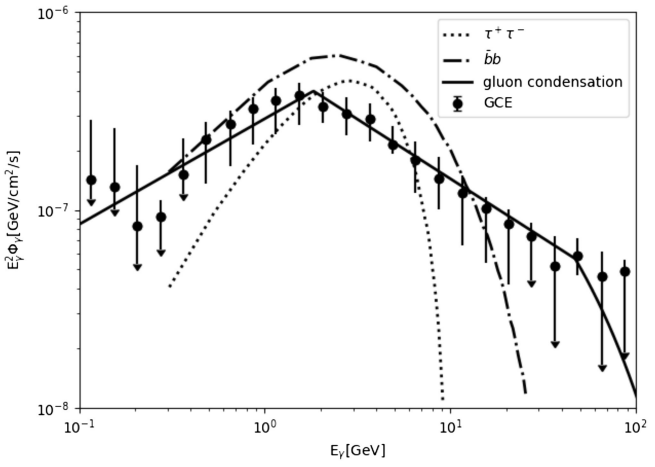

FIG. 3. A comparison of the GCE spectra between the gluon condensation mechanism with the dark matter model, the latter is taken from [30] and the curve heights have been adjusted.

An important characteristic of the gluon condensation mechanism is that its spectrum presents a straight line in a double logarithmic coordinator within an interval $[E_\pi^{\rm GC}, E_\pi^{\rm cut}]$. Besides, the length of the linear interval increases with $(E_\pi^{\rm GC})^2$. We compare it with a dark matter annihilation model [30]. The shape of the dark matter annihilation spectrum is usually parameterized by a power law with an exponential cutoff $\Phi = K(E_\gamma/E_0)^{-\Gamma}\exp(-E_\gamma/E_{\rm cut})$, which is different from the gluon condensation mechanism. The difference between the two can be clearly seen in Fig. 3.

IV. NONROTATING NEUTRON STARS

The measured spectra shown in Fig. 1 have some differences between each other since they are derived by different analysis processes. However, each of these spectra is a synthesis of the sub-spectra of many sources. Curiously each of them exhibits the typical BPL form. We know that it is mathematically almost impossible to synthesize several different BPL curves into one simple BPL. This requires us to make new considerations about the sources of the spectra in Fig. 1.

Using the bright low-mass x-ray binaries population to estimate the number of millisecond pulsars, Cholis, Hooper, and Linden have found millisecond pulsars is not enough to explain the whole excess [31]. However, it is also highly depended on the luminosity function of millisecond pulsars. Dinsmore and Slatyer have examined the luminosity function of millisecond pulsars to explain GCE and found the needed number of millisecond pulsars should be in the range of $\mathcal{O}(10^{4-5})$ [14]. Another possible suggestion that the GCE originates from currently undetected neutron stars with the similar spatial distribution of millisecond pulsars. The nonrotating (or slower rotating) neutron star is hard to be detected which makes it a possible candidate. In this work, we attempt to use the gluon condensation effect of the nonrotating (or slower rotating) neutron stars to explain the GCE.

The Galactic Center is a fascinating and mysterious place, filled with high-density materials such as neutron stars and black holes. When a giant star burns up its nuclear

fuel, its core collapses into a very compact sphere, causing its rotation speed to increase rapidly due to the angular momentum conservation. These rotating stars emit pulsed electromagnetic waves that have been identified as pulsars. Theoretically, not all neutron stars are the pulsars. At the beginning of the formation of a neutron star, its rotation energy may be seriously lost due to other reasons, for say, abandonment of a large number of neutron materials, forming an nonrotating neutron star.

Nonrotating neutron stars do not have characteristic pulse electromagnetic radiation, making them difficult to distinguish from other dark stars. Nevertheless, the theoretical study of nonrotating neutron stars is still an interesting topic. Let us give a few examples. As early as 1941, Cowling provided the first classification of modes according to the physics dominating their behavior [32]. Gittins and Andersson discussed the r-modes of slowly rotating, stratified neutron stars [33]. The mass and radius of nonrotating neutron star with maximum mass play a crucial role in constraining the elusive equation of state of cold dense matter and in predicting the fate of remnants from binary neutron star mergers [34].

We only focus on the contribution of the nonrotating neutron stars to the GCE and hope it can provide indirect evidence of existing nonrotating neutron stars in the Galactic Center. The spatial morphology of the GCE requires the existence of a population of almost spherically symmetric distribution of nonrotating neutron stars at the Galactic Center. We image that neutron stars are formed by the collapse of massive stars, in which high and low rotational (the latter including nonrotating) neutron stars are produced randomly, mainly determined by whether the stars have large primordial angular momentum. If these nonrotating neutron stars are old neutron stars and originate from early stars, they would have the similar spatial distribution of millisecond pulsars which is approximately symmetric spatial distribution. We emphasize that since there is no direct detection of the nonrotating neutron stars, the above mentioned origin and spatial morphology is an assumption.

When the VHE protons in the Galactic Center collide with these nonrotating neutron stars, they generate gamma rays with a BPL shape, as predicted by the gluon condensation mechanism. The pA^* collisions generate spectra peaked around $\sim$1 GeV. However, nonrotating neutron star loses its rotational acceleration, and the high-energy protons are not accelerated by the star's rotating electromagnetic fields. Most of these protons are cosmic-ray protons that have been further accelerated by known or unknown mechanisms in the Galactic Center. Since these accelerators are shared by nonrotating neutron stars within the observation area of each set in Fig. 1, the colliding protons have the same global power index β_p in Eq. (8). Similarly, where the parameter β_γ describes photon loss during flight in a considerable measurement area of the Galactic Center, and it is also a constant for the same reason. The gluon condensation spectra in Eq. (8) has only four parameters, and the remaining parameter C_γ is determined by the strength of the gamma rays. Consequently, we can observe a total spectrum with a broken power law as shown in Fig. 1.

V. DISCUSSIONS AND SUMMARY

Why we have not considered the contributions of the "π-bump" in the traditional hadronic mechanism at $E_\gamma \sim 1$ GeV ? In normal hadronic collisions, a significant portion of the proton's kinetic energy is used to heat secondary particles without the gluon condensation effect. However, with the gluon condensation effect, almost all of the available energy at the c.m. frame is utilized to create prions and follow gamma rays. Therefore, the traditional π-bump near $E_\gamma \sim 1$ GeV without the gluon condensation effect is covered by the GC spectra in Fig. 1.

We estimate the contributions of the gluon condensation mechanism to the Milky Way's diffuse emission along the Galactic plane if considering the VHE cosmic protons colliding with molecular hydrogen of the interstellar medium. the gluon condensation threshold $E_\pi^{\rm GC} \sim 10$ TeV for the pp or p-light nuclei collisions, which is determined by the value of x_c [29]. Using Eqs. (9) and (10), one can find that it requests $E_p^{\rm GC} > 10^4$ PeV, which exceeds the limit of the proton acceleration mechanism in our Milky Way.

In summary, the intrinsic GCE spectra present the BPL shape. We propose a novel interpretation on the origin of the GCE, focusing on the observed spectral shape. Protons are accelerated at the Galactic Center and collide with the neutron cluster on the surface of the nonrotating neutron stars. Due to the gluon condensation in nucleons, these collisions produce a large number of mesons, which have reached the saturation state and subsequently generate the BPL in the gamma ray spectra.

ACKNOWLEDGMENTS

This work is supported by the National Natural Science Foundation of China (NNSFC) No. 11851303 and No. 12003069, the National Key Research and Development Program of China No. 2022YFF0503304.

[1] L. Goodenough and D. Hooper, Possible evidence for dark matter annihilation in the inner Milky Way from the Fermi gamma ray space telescope, arXiv:0910.2998.

[2] D. Hooper and L. Goodenough, Dark matter annihilation in the Galactic Center as seen by the Fermi gamma ray space telescope, Phys. Lett. B **697**, 412 (2011).

[3] C. Gordon and O. Macias, Dark matter and pulsar model constraints from Galactic Center Fermi-LAT gamma ray observations, Phys. Rev. D **88**, 083521 (2013); **89**, 049901 (E) (2014).

[4] S. Murgia, The Fermi-LAT Galactic Center excess: Evidence of annihilating dark matter?, Annu. Rev. Nucl. Part. Sci. **70**, 455 (2020).

[5] D. Hooper, The status of the Galactic Center gamma-ray excess, SciPost Phys. Proc. **12**, 006 (2023), arXiv:2209.14370.

[6] S. Walsh, S. McBreen, A. Martin-Carrillo, T. Dauser, N. Wijers, J. Wilms, J. Schaye, and D. Barret, Detection capabilities of the Athena X-IFU for the warm-hot inter-Galactic medium using gamma-ray burst x-ray afterglows, Astron. Astrophys. **642**, A24 (2020).

[7] C. Gordon and O. Macias, Dark matter and pulsar model constraints from Galactic Center Fermi-LAT gamma-ray observations, Phys. Rev. D **88**, 083521 (2013).

[8] K. N. Abazajian, N. Canac, S. Horiuchi, and M. Kaplinghat, Astrophysical and dark matter interpretations of extended gamma-ray emission from the Galactic Center, Phys. Rev. D **90**, 023526 (2014).

[9] F. Calore, I. Cholis, and C. Weniger, Background model systematics for the Fermi GeV excess, J. Cosmol. Astropart. Phys. 03 (2015) 038.

[10] M. Ajello *et al.*, Fermi-LAT observations of high-energy γ-ray emission toward the Galactic Center, Astrophys. J. **819**, 44 (2016).

[11] M. Ackermann *et al.*, The Fermi Galactic Center GeV excess and implications for dark matter, Astrophys. J. **840**, 43 (2017).

[12] Y. M. Zhong, S. D. McDermott, I. Cholis, and P. J. Fox, Testing the sensitivity of the Galactic Center excess to the point source mask, Phys. Rev. Lett. **124**, 231103 (2020).

[13] M. D. Mauro, Characteristics of the Galactic Center excess measured with 11 years of Fermi-LAT data, Phys. Rev. D **103**, 063029 (2021).

[14] J. T. Dinsmore and T. R. Slatyer, Luminosity functions consistent with pulsar-dominated Galactic Center excess, J. Cosmol. Astropart. Phys. 06 (2022) 025.

[15] M. Ackermann *et al.*, Detection of the characteristic pion-decay signature in supernova remnants, Science **339**, 807 (2013).

[16] A. Szczurek, From unintegrated gluon distributions to particle production in hadronic collisions at high energies, in *Proceedings of the XI International Workshop on Deep Inelastic Scattering, St. Petersburg*, (2003), arXiv:hep-ph/0309146.

[17] L. McLerran, The CGC and the glasma: Two lectures at the Yukawa Institute, Prog. Theor. Phys. Suppl. **187**, 17 (2011).

[18] W. Zhu, A new approach to parton recombination in the QCD evolution equations, Nucl. Phys. **B55**, 245 (1999).

[19] W. Zhu, Z. Q. Shen, and J. H. Ruan, Can a chaotic solution in the QCD evolution equation restra in high-energy collider physics?, Chin. Phys. Lett. **25**, 3605 (2008).

[20] W. Zhu, Z. Shen, and J. Ruan, The chaotic effects in a nonlinear QCD evolution equation, Nucl. Phys. **B911**, 1 (2016).

[21] W Zhu and J. Lan, The gluon condensation at high energy hadron collisions, Nucl. Phys. **B916**, 647 (2017).

[22] F. A. Aharonian, *Very High Energy Cosmic Gamma Radiation: A Crucial Window on the Extreme Universe* (World Scientific Publishing, Singapore, 2004), 10.1142/4657.

[23] L. V. Gribov, E. M. Levin, and M. G. Ryskin, Semihard processes in QCD, Phys. Rep. **100**, 1 (1983).

[24] A. Szczurek, From unintegrated gluon distributions to particle production in nucleon-nucleon collisions at RHIC energies, Acta Phys. Pol. B **34**, 3191 (2003), arXiv:hep-ph/0304129.

[25] W. Zhu, J. Lan, and J. Ruan, The gluon condensation in high energy cosmic rays, Int. J. Mod. Phys. E **27**, 1850073 (2018).

[26] L. Feng, J. H. Ruan, F. Wang, and W. Zhu, Looking for the gluon condensation signature in protons using the Earth-limb gamma-ray spectra, Astrophys. J. **868**, 2 (2018).

[27] J. Ruan, Z. Zheng, and W. Zhu, Exploring the possible gluon condensation signature in gamma-ray emission from pulsars, J. Cosmol. Astropart. Phys. 08 (2021) 065.

[28] Z. C. Zou, T. F. Huang, C. M. Li, H. R. Zheng, and W. Zhu, Gluon condensation signature in the GeV gamma-ray spectra of pulsars, Phys. Rev. D **107**, 063032 (2023).

[29] W. Zhu, Q. Chen, Z. Cui, and J. Ruan, The gluon condensation in hadron collisions, Nucl. Phys. **B984**, 115961 (2022).

[30] M. D. Mauro, The characteristics of the Galactic Center excess measured with 11 years of Fermi-LAT data, Phys. Rev. D **103**, 063029 (2021).

[31] I. Cholis, D. Hooper, and T. Linden, Challenges in explaining the Galactic Center gamma-ray excess with millisecond pulsars, J. Cosmol. Astropart. Phys. 06 (2015) 043.

[32] T. G. Cowling, The nonradial oscillations of polytropic stats, Mon. Not. R. Astron. Soc. **101**, 367 (1941).

[33] F. Gittins and N. Andersson, *r*-modes of slowly rotating, stratified neutron stars, Mon. Not. R. Astron. Soc. **521**, 3043 (2023).

[34] S. P. Tang, B. Gao, Y. J. Li, Y. Z. Fan, and D. M. Wei, Measuring mass and radius of the maximum-mass non-rotating neutron star, arXiv:2309.15441.